Journal of Non-Crystalline Solids 427 (2015) 120–133

Contents lists available at ScienceDirect

Journal of Non-Crystalline Solids

journal homepage: www.elsevier.com/locate/jnoncrysol

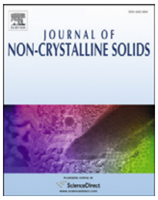

Phase separation and crystallization effects on the structure and durability of molybdenum borosilicate glass

Elodie Nicoleau [a], Sophie Schuller [b], Frédéric Angeli [a,*], Thibault Charpentier [c], Patrick Jollivet [a], Alexandre Le Gac [a], Maxime Fournier [a], Adel Mesbah [d], Filipe Vasconcelos [c]

[a] CEA, DEN, DTCD, SECM, LCLT, F-30207 Bagnols-sur-cèze, France
[b] CEA, DEN, DTCD, SECM, LDMC, F-30207 Bagnols-sur-cèze, France
[c] CEA, IRAMIS, NIMBE, LSDRM, UMR CEA/CNRS 3685, F-91191 Gif-sur-Yvette cedex, France
[d] ICSM, UMR 5257 CEA/CNRS/UM2/ENSCM, F-30207 Bagnols-sur-cèze, France

ARTICLE INFO

Article history:
Received 2 March 2015
Received in revised form 23 June 2015
Accepted 2 July 2015
Available online 30 July 2015

Keywords:
Borosilicate glass;
Structure;
Phase separation;
Crystallization;
Molybdenum;
Chemical durability

ABSTRACT

The effects of phase separation by nucleation and growth as well as those of crystallization on the structure and the chemical durability of sodium borosilicate glasses enriched in molybdenum oxide were investigated. Increasing concentrations of MoO_3 (0 to 10% molar) were added to glasses which were homogeneous ($MoO_3 \leq 1.4\%$ molar) or with crystallizations and separated phases ($MoO_3 > 1.4\%$ molar). Their structure was determined by ^{11}B, ^{23}Na, ^{29}Si and ^{95}Mo MAS NMR, and ^{23}Na MQMAS NMR, coupled with DFT calculations of NMR parameters. Their microstructure and morphology were characterized by X-ray diffraction and by electronic microscopy. These complementary approaches pointed out a decrease in the number of non-bridging oxygens (NBOs) within the vitreous matrix, first initiated by an increase in polymerization for glasses with a low molybdenum oxide content (<2 % molar), and combined with the decrease in the number of tetrahedral boron for higher contents. Correlations between the chemical durability, the structure and the microstructure of the glasses were then obtained at low and high dissolution reaction progress. The modifications to the chemical composition and to the structure of the surrounding glass induced by increasing MoO_3 strongly influenced the matrix durability. Moreover, the nature and the morphology of the separated phases influence the dissolution kinetics by modifying the solution chemistry.

1. Introduction

The phase separation and crystallization processes within glasses modify their physico-chemical properties (viscosity, thermal dilatation, crystallization behavior, chemical durability) [1]. Controlling phase separation enables a wide variety of heterogeneous materials to be fabricated, opening up a broad range of industrial applications (Pyrex, Vycor, opal glass, porous glass) [2–4]. While such mechanisms may be considered to be advantageous in vitroceramics, they can however deteriorate the quality of the material if they are not controlled. For example, phase separation obtained by a heat treatment of nucleation and growth [1,5–7] or by the addition of nucleating agents [8,9] to sodium borosilicate glasses modifies glass behavior in an aqueous medium.

Depending on the nature, the composition and the morphology of the separated phases formed, demixed glasses can be more or less durable compared to the initial homogeneous glasses. Ternary glass compositions (SiO_2–Na_2O–B_2O_3) with a miscibility gap, for example, enable demixed glass compositions (e.g., Vycor), which are easily leached. This type of phase separation is on the other hand to be avoided when highly durable glass is required, for radioactive waste conditioning glass for geological disposal [10,11].

Borosilicate glasses demixed by the addition of molybdenum oxide represent a model simplified system for investigating heterogeneous glasses. Molybdenum is a fission product coming from spent fuel reprocessing solutions, and is weakly soluble in glass [12–15]. When the content is higher than its solubility limit, processes of phase separation and of crystallization lead to the formation of heterogeneous glasses [16]. Several authors have pointed out the influence of molybdenum oxide on the structure and microstructure of sodium borosilicate glasses. Initiated by a liquid–liquid phase separation at high temperature, separated phases enriched in molybdenum oxide crystallize during cooling [14,17,18], giving partially crystallized heterogeneous material containing alkali and alkaline-earth molybdates.

It has been suggested that these mechanisms occur at an atomic scale by the clustering of several isolated molybdate units. Molybdenum, mainly under its oxidation state + VI in glasses prepared in oxidizing conditions [16,19–21], is found in the form of MoO_4^{2-} tetrahedral units distributed in depolymerized areas of glass with charge-compensating cations (for example alkalis and alkaline-earths). This

---

[*] Corresponding author.
E-mail address: frederic.angeli@cea.fr (F. Angeli).

http://dx.doi.org/10.1016/j.jnoncrysol.2015.07.001
0022-3093/

molybdenum structural environment leads to a repolymerization of the remaining silicate network [22,23] following the equation:

$$MoO_3 + \left(2Q^3, Ca^{2+} \text{ or } 2Na^+\right) \rightarrow \left(MoO_4^{2-}, Ca^{2+} \text{ or } 2Na^+\right) + 2Q^4.$$

In soda-lime borosilicate glass, the nature of the separated phases and of the crystalline phases depends on the charge compensator cation of the molybdates. It has been shown that the quantity of Na^+ remaining in the glass network after compensation for the BO_4^- units governs the local environment of the molybdate units and thus the nature of the phases formed during the process of phase separation and crystallization. The decrease in the number of "free" Na^+ ions – induced by the gradual increase of CaO and B_2O_3 content – leads to the formation of partially crystallized glasses containing a mixture of Na_2MoO_4 and $CaMoO_4$ phases, or $CaMoO_4$ only, depending on the glass composition [18,22,24]. Greater understanding of the chemical durability properties of this type of glass can be addressed by investigations of its structural and morphological changes.

In this work, a series of borosilicate glasses with varying molybdenum oxide contents were studied. The glasses contained enough sodium to compensate $[BO_4]^-$ and $[MoO_4]^{2-}$ units, and to form sodium molybdates during the phase separation and crystallization processes. The addition of increasing concentrations of MoO_3 (0 to 10% molar) enabled the fabrication of either glasses which were homogeneous at nanometric scale (MoO_3 content <1.4% molar), or glasses containing separated phases at a microscopic or macroscopic scale when the molybdenum oxide content was high (>2% molar). Using complementary approaches with solid-state high resolution nuclear magnetic resonance (^{11}B, ^{23}Na, ^{29}Si, ^{95}Mo), high resolution transmission electron microscopy (HRTEM) and X-ray diffraction with Rietveld refinement, it becomes possible to give a detailed description of the structural, morphological and microstructural evolution of glasses. All the glasses were leached in deionized water at pH 9 and at 90 °C, following different alteration regimes (short and medium term). These approaches give further insights into the aqueous reactivity of homogeneous vitreous matrices containing varying amounts of phases whose chemical and/or geometric nature differ.

2. Experimental procedure

2.1. Glass preparation

A series of molybdenum-bearing sodium borosilicate glasses (*x*Mo) in which the molybdenum oxide proportionally replaced other oxides following the formula $((100x)\ 63SiO_2 - 17B_2O_3 - 20Na_2O) - xMoO_3$ with $x = 0, 0.5, 0.8, 2, 3, 4, 5$ and 10 were investigated. The glasses were prepared by mixing appropriate quantities of the precursors SiO_2, H_3BO_3, Na_2CO_3 and MoO_3. The powder mixtures were then melted at 1250 °C for 3 h in Pt–Rh crucibles, then poured and cooled between two copper plates with a cooling rate between 10^2 °C·min^{-1} and 10^3 °C·min^{-1} [16,25]. The glass chemical compositions were checked by alkaline fusion followed by an analysis with inductively coupled plasma-optical emission spectroscopy (ICP-OES). The analyses gave the theoretical composition at less than 0.5% of nominal compositions listed in Table 1.

Table 1
Nominal composition of the *x*Mo glass series in % molar.

Glass	0Mo	0.5Mo	0.8Mo	2Mo	3Mo	4Mo	5Mo	10Mo
SiO_2	63.5	63.2	63.0	62.2	61.1	61.0	60.3	57.1
B_2O_3	16.9	16.8	16.8	16.6	16.5	16.2	16.1	15.2
Na_2O	19.6	19.5	19.4	19.2	19.4	18.8	18.6	17.6
MoO_3	–	0.5	0.8	2.0	3.0	4.0	5.0	10.0

2.2. Solid characterization methods

2.2.1. Powder X-ray diffraction (PXRD)

After cooling, all the glass samples were characterized by powder X-ray diffraction (PXRD) using the PANalytical X'Pert Pro diffractometer equipped with a solid detector X'Celerator and using Cu $K\alpha_{1,2}$ radiation ($\lambda = 1.54184$ Å). All the PXRD patterns were collected in the Bragg–Brentano geometry in the angular range of $10° < 2\theta < 80°$, with a step size $\Delta 2\theta = 0.017°$ and total counting time of at least 5 h. PXRD of pure silicon (Si) was collected in the same condition and used to extract the instrumental function. Moreover, a known amount of Si was also mixed to each phase and used as internal standard to quantify the amount of crystallized phase vs amorphous. Besides the Si, the crystalline phases present in each PXRD were identified by comparison with the International Center for Diffraction Data.

After that, all the PXRD patterns were refined by the Rietveld method using the "Fullprof_suite" program [26]. During the refinement, different parameters were allowed to vary: zero shift, scale factors, preferred orientation, asymmetry parameters, lattice parameters, a global thermal displacement for each phase, and intrinsic microstructure parameters to extract size effect.

The solubility limit of the molybdenum oxide and the presence of a low crystalline phase content in the glasses were also checked by dissolution heat measurement with a CALSOL calorimeter [27].

2.2.2. Solid-state nuclear magnetic resonance

The spectra were collected on a Bruker Avance II 500WB spectrometer operating at a magnetic field of 11.72 T. ^{11}B, ^{23}Na and ^{29}Si MAS NMR spectra were acquired using a Bruker CPMAS probe (with ZrO_2 rotor, outer diameter (OD) 4 mm) at a sample rotation frequency of 14 kHz for all nuclei. For ^{95}Mo, a Bruker CPMAS probe with 7 mm (OD) ZrO_2 rotor was used at a spinning frequency of 6 kHz.

2.2.2.1. ^{11}B MAS NMR. To ensure spectrum quantitativeness, a short pulse of 1 μs (tip angle of π/12) [30] and a recycle delay of 2 s were used. Chemical shifts were referenced to an external sample of 1 M boric acid solution (19.6 ppm relative to the boron trifluoride etherate).

2.2.2.2 . ^{29}Si MAS NMR. Silicon spectra were acquired using the CPMG sequence [28], by typically accumulating 32 echoes with an echo delay of 2.4 ms between consecutive 180° pulses. The echoes were then summed and Fourier transformed to obtain the spectra shown. A 20 s recycling time was used; checks were carried out on two glass samples that no spectral deformation could be observed for longer recycling delays (200 s and 1200 s). The spectra were referenced to an external tetrakis(trimethylsilyl)silane (TKS) sample for which the highest-intensity peak is situated −9.9 ppm from that of TMS.

2.2.2.3. ^{23}Na MAS and MQMAS NMR. A short pulse (π/12 with a pulse width of 1 μs) and a recycle delay of 1 s were used for the MAS spectra. ^{23}Na MQMAS spectra were acquired with a RIACT-II two-pulse sequence [29] with optimized excitation and reconversion pulses of $p_1 = 7$ μs and $p_2 = 18$ μs respectively (*rf* field strength of 80 kHz, the second pulse length matched one quarter of the rotation period), and 64 t_1 increments of 10 μs were acquired. ^{23}Na chemical shifts were referenced to an external sample of 1 M NaCl (0 ppm).

2.2.2.4. ^{95}Mo MAS NMR. A spin echo pulse sequence with a rotor-synchronized echo delay of one rotation period was used with a recycle delay of 1 s. Because of its low sensitivity (natural abundance of 15.9%, Larmor frequency of 32.5 MHz), typically 100,000–200,000 scans were accumulated. The moderate value of its nuclear quadrupolar moment ($Q = -2.2 \cdot 10^{-30}$ m^2), combined with its nuclear spin ($I = 5/2$), enabled the use of bigger 7 mm rotor to increase the sample volume for a better signal-to-noise ratio. ^{95}Mo chemical shifts were referenced